Journal of Cleaner Production 238 (2019) 117998

Contents lists available at ScienceDirect

Journal of Cleaner Production

journal homepage: www.elsevier.com/locate/jclepro

# Multiscale recycling rare earth elements from real waste trichromatic phosphors containing glass

Hu Liu [a, *], Shiyin Li [a], Bo Wang [a], Kun Wang [a], Ruize Wu [a], Christian Ekberg [b], Alex A. Volinsky [c]

[a] School of Materials Science and Engineering, Nanchang University, 330031, Nanchang, PR China
[b] Nuclear Chemistry and Industrial Materials Recycling, Department of Chemistry and Chemical Engineering, Chalmers University of Technology, 41296, Gothenburg, Sweden
[c] Department of Mechanical Engineering, University of South Florida, Tampa, FL, 33620, USA

ARTICLE INFO

*Article history:*
Received 12 January 2019
Received in revised form
7 June 2019
Accepted 10 August 2019
Available online 10 August 2019

Handling Editor: CT Lee

*Keywords:*
Recyle
Rare earth
Waste phosphors
Glass
Effctive
Economical

ABSTRACT

In this study, desilication, decomposition, and acidolysis were used to recycle rare earth elements (REEs) from real waste trichromatic phosphors containing glass at laboratory and pilot plant scales. The effects of pre-sintering temperature, sieving, alkaline leaching conditions and alkaline fusion temperature on removal of glass and recovery of REEs were investigated. About 88% of glass fragments in the original matrix were removed after dry sieving through a 0.05 mm mesh sieve and leaching by 5 mol/L NaOH solution at 90 °C for 4 h at the appropriate 5:1 liquid-solid ratio. The blue and green phosphors were decomposed by alkaline fusion at 600 °C for 2 h. Y, Eu, Ce and Tb-rich solutions were respectively obtained by the two-steps acidolysis. The total leaching rate of REEs reached 94%, while the rates of Y, Eu, Ce, and Tb were 96%, 99%, 81%, and 92%, respectively. Furthermore, in the ton level industrial pilot, the successful application of this approach increased the recovery of the REEs up to 90% compared with the existing technology. Except for the fixed capital investments and taxes, this approach showed positive economic feasibility, since the savings are 1115 €/ton. Therefore, recycling of REEs from waste phosphors is one of the cleaner and economical ways to balance the demand and supply of REEs outside of China.


## 1. Introduction

The rare earth elements (REEs), especially Tb and Eu, are considered the most critical materials by the European Union (European Commission, 2017). Coupled with the limited supply, market availability and significant price fluctuations (Mancheri, 2015), there are still significant technical and economic challenges to create substantial REEs supply chains outside of China in the next ten years (Goodenough et al., 2018). Mining from deposits brings environmental problems caused by ammonia nitrogen and heavy metals (Tang et al., 2018). Therefore, aside from primary mining, recycling REEs from the end-of-life goods is one of the most useful pathways to ensure an independent supply for future applications (Binnemans et al., 2015; Ali et al., 2017). Recycling secondary resources can reduce the environmental pollution and costs (Kumari et al., 2018; Pellegrini et al., 2017).

Many studies have been conducted on recycling REEs from waste, with a particular focus on lamp phosphors (Jowitt et al., 2018). Phosphors in compact fluorescents are a rich source of the critical and highly valued elements, including Y, Ce, Tb and Eu, which are retained in red phosphor ($Y_2O_3$: Eu, YOX), blue phosphor ($BaMgAl_{10}O_{17}:Eu^{2+}$, BAM) and green phosphor ($CeMgAl_{11}O_{19}:Tb^{3+}$, CTMA or $LaPO_4:Ce^{3+}$, LAP), and the REEs content is 10–20% (Lederer et al., 2017). Due to the long-term exposure to UV radiation and bombardment by mercury atoms and ions, the phosphors are contaminated by mercury after a long-time continuous use (Aljerf and Al Masri, 2018; Tanaka et al., 2013). Most of the mercury absorbed by phosphors (Jang et al., 2005) is typically carried out thermally by distillation (Chang et al., 2009). For a complete removal of glass-bound mercury, 800 °C treatment for several hours is often needed. However, due to mercury vapor contamination, it is not quite desirable. Thus, wet decontamination routes have also been investigated. Oxidative leaching using sodium hypochlorite or iodine in potassium iodide ($I_2$/KI) has shown high leaching efficiency of mercury, while leaving the REEs in the

* Corresponding author.
*E-mail address:* liuhu@ncu.edu.cn (H. Liu).

https://doi.org/10.1016/j.jclepro.2019.117998
0959-6526/

residue (Tunsu et al., 2015; Coskun and Civelekoglu, 2015).

Hydrometallurgy is a traditionally established and easy method for the recovery of REEs from waste phosphors, and pyrometallurgical pretreatments are used to aid REEs leaching. Some of the 2014–2019 representative studies and the corresponding achieved results are presented in Table 1. Since red phosphor ($Y_2O_3$: Eu, YOX) is an oxide that is easy to leach, Y and Eu have been intensively recovered and even regenerated into new red phosphor (Tunsu et al., 2016). However, blue (BAM) and green phosphors (CTMA or LAP) are difficult to dissolve due to their stable crystal structure. These structures lead to high chemical stability and high energy input requirements to break the chemical bonds; therefore, blue and green phosphors show high resistance to acid attack. However, they are sensitive to the effects of alkaline fusion (NaOH at 800 °C, $Na_2CO_3$ at 1000 °C, $Na_2O_2$ at 650 °C, or $Ba(OH)_2$ at 950 °C), mechanical activation (high-energy milling), or mechano-chemical treatment (milling-leaching). Alkaline fusion is used to decompose blue and green phosphors into oxides, which can be leached under mild conditions. Mechanical activation (high-energy milling) causes changes in the crystallite surface and induces strain in the crystal lattice, resulting in a disordered crystal structure, which extensively accelerates the subsequent leaching operation and thus avoiding the need for thermal activation (Tan et al., 2016, He et al. (2018)). Since some defects are not stable and have short relaxation time, highly excited states decay before the leaching stage is initiated (Balaz et al., 2013). The process of mechanical activation followed by leaching only utilizes the long-lived excited states. Therefore, Van et al. combined milling and leaching, called the mechano-chemical process, where all excited states are used, including the short-lived states. The activated outer shell of the particle can be simultaneously leached, thereby exposing fresh surface and improving the leaching performance (Van Loy et al. (2018)). Bioleaching is considered as an eco-friendly alternative to the currently applied methods that use strong inorganic acids, but its leaching efficiency is currently less than 15% (Hopfe et al., 2017, 2018; Reed et al., 2016). Above all, the current technical routes could be classified into four categories, (1) direct leaching, (2) Mechanochemical-assisted leaching, (3) Alkaline fusion and leaching, and (4) Bioleaching. From the perspective of industrialization (large-scale and low cost), alkaline fusion and leaching is probably more likely to be used to recycling REEs from waste phosphors.

Multiple literature reports dealt with the laboratory-scale research of REEs recycling from waste phosphor powders or pure phosphors. Processes for waste phosphor powders with glass, such as alkaline fusion and mechano-chemical-assisted leaching, have a relatively high energy consumption due to high calcination temperature or high milling speed, including desilication, decomposition, and acidolysis. It should be noted that alkaline fusion leads to the formation of silicates due to the presence of fine glass particles, which is seldom discussed by researchers. During the following leaching, $SiO_3^{2-}$ is easily transformed into $H_2SiO_4^{2-}$, $H_3SiO_4^-$ and $H_4SiO_4$ through the hydrolysis reaction (1), then turn into network structure through the -Si-O-Si- linkage as reaction (2) (Coradin et al., 2002).

$$3SiO_3^{2-} + 3H_2O + 3H^+ \rightarrow H_2SiO_4^{2-} + H_3SiO_4^- + H_4SiO_4 \quad (1)$$

$$H_2SiO_4^{2-} + H_4SiO_4 + 2H^+ \rightarrow (OH)_3\,Si\,O\,Si\,(OH)_3 + H_2O \quad (2)$$

Isolated Ludox particles and aggregates made of silica particles are bound to the polypeptide chain via the $Si{-}O^-/RE^{3+}$ electrostatic interactions. This can be ascribed to the interaction of the counterion ($RE^{3+}$ or other cations in the solution) with the surface or some anions in the solution. The RE ions can come into close contact with the surfaces of Ludox particles and neutralize their negative charge. As a result, the silica aggregates containing REEs become a deposit, which reduces the recovery of REEs.

In order to increase the recovery of REEs from real waste trichromatic phosphors containing glass, and reduce the cost, improved processes, including desilication, decomposition and acidolysis were synthetically investigated during REEs recycling from real waste trichromatic phosphors at the laboratory (g and kg sample size) and pilot plant (metric ton sample size) scales in this paper. Economic assessment and technical feasibility, along with the ecological aspects are briefly discussed.

## 2. Materials and methods

### 2.1. Materials

Real waste trichromatic phosphors (WTP) used in experiments were supplied by the Xinli Co. Ltd from Guangzhou, China. The chemical composition always varies between different batches of waste phosphors. The waste phosphors used in the laboratory and pilot plant scale experiments were from the same batch. They have been processed by the homogenization treatment and packed. For the laboratory experiment, ten samples were collected from ten packs (25 kg/pack) in different layers, respectively, by random sampling, 500 g each. Then the samples were manually blended. The WTP mainly contains fine trichromatic phosphors (YOX, BAM, and CTMA), glass fragments and flocculent organics (possibly from the package).

### 2.2. Proposed process flow

The process to recover REEs from WTP follows the flowchart shown in Fig. 1. The process mainly includes the six following steps.

(1) Burn off flocculent organics. The WTP was calcinated at 200–600 °C for 2 h, since flocculent organics were detrimental to separate the glass fragments by sieving.
(2) Remove large size glass fragments. Waste samples were dry sieved (38 μm, 50 μm, 74 μm, and 150 μm mesh sizes, respectively) and the particle size distribution was determined by weighing the collected sieved fractions.
(3) Selective leaching of red phosphors (YOX) was carried out with HCl at 60 °C for 4 h at the optimized conditions: 4M HCl and 3:1 liquid-solid ratio, as described in the previous study (Liu et al., 2014). After filtration, Y and Eu-rich solution was obtained as filtrate 1, and the residue 1 was dried at 100 °C.
(4) Remove fine glass. Leaching of fine glass was carried out with NaOH solution (1.25 M, 2.5 M, 3.75 M, 5 M, and 6.25 M) at 90 °C for 4 h. After filtration, residue 2 was dried at 100 °C.
(5) Decomposition of BAM and CTMA. Residue 2 and NaOH were mixed with 1:1 wt ratio. The mixture was placed into 100 ml iron crucibles. Sintering was performed in a furnace at 200–900 °C for 2 h. In order to remove $NaAlO_2$ generated during the alkaline fusion, the products were cleaned by deionized water (5:1 liquid-solid ratio) at 60 °C for 2 h twice. The insoluble matter was filtered and dried at 100 °C.
(6) Leaching of REEs from washed fusion products. The washed products were leached by 5M HCl at 60 °C for 2 h (Liu et al., 2014). After filtration, Ce and Tb-rich solution was obtained as filtrate 3.

To reduce the possibility of REEs loss, extra deionized water was used to clean the samples during filtration. In the end, two mixed REEs oxides were prepared by precipitating with oxalic acid, followed by thermal treatment of oxalates at 800 °C.

**Table 1**
Various processes reported for recovering REEs.

| Targeted REEs | Raw materials | Processes | Results | References |
|---|---|---|---|---|
| Y, Eu, Tb, Ce, La and Gd | Waste phosphors | Leaching and solvent extraction | The total recovery yields were: 93% Y, 90% Eu, 77% Tb, 60% for Ce and 50% for La and Gd. | Innocenzi et al. (2018) |
| Ce, Tb and Eu | BAM and CTMA phosphors | Alkaline fusion and leaching | The maximum leaching rate of Ce (96.47%), Tb (92.23%) and Eu (82.43%), and the RE oxides (94.12%) were obtained. | Yu et al. (2018) |
| Y and Eu | Waste phosphors | Bioleaching | Highest leaching results with K. xylinus, L. casei and Y. lipolytica (up to 12.6%). The oxidic red phosphor was preferably leached. | Hopfe et al. (2018) |
| La and Ce | Green phosphor, $LaPO_4:Ce^{3+}$ | Mechanochemical-assisted leaching | 98% recovery of REEs at room temperature after cycled mechanical activation. | Van Loy et al. (2018) |
| Y, Eu, Tb, La and Ce | Waste phosphors | Mechanochemical treatment and leaching | The chelator-induced leaching yield (%) of REs was enhanced significantly by wet milling (Ce, $60.5 \pm 6.6$; Eu, $84.1 \pm 1.5$; La, $53.1 \pm 4.9$; Tb, $56.5 \pm 3.7$; Y, $83.8 \pm 2.3$). | Hasegawa et al., (2018) |
| Ce and Tb | Waste phosphors | Alkali mechanical activation | The leaching rates of Ce and Tb reach 85% and 89.8%, respectively due to the changes caused by the destruction of the spinel structure. | He et al. (2018) |
| Y, Eu, Tb, La, Gd and Ce | Waste phosphors | Thermal pretreatment, alkaline fusion and leaching | The extraction yields were: 99% for Y and Eu, 80% for Tb, 65% for La, 63% for Gd and 60% for Ce. | Ippolito et al., 2017 |
| Y and Eu | Waste phosphors | Bioleaching | The leaching rates ranged between 6.7 and 12.5 mol-% for Y and 5.5 and 12.1 mol-% for Eu. All other elements were released in only very small amounts by the microorganisms or its supernatant. | Hopfe et al., (2017) |
| Y, Tb, La, Ce and Eu | Waste phosphors | Mechanical activation and leaching | The leaching rates of Tb, La and Ce had a significant enhancement of around 90%; and the leaching rates for Eu and Y were 93.1% and 94.6%. | Tan et al., 2017 |
| Y and Eu | Waste phosphors | Leaching and solvent extraction | The leaching rate of Y and Eu was higher than 95%, an oxide containing 99.96% REEs, of which 94.61% was Y and 5.09% was Eu, was obtained. | Tunsu et al., (2016) |
| Y, Eu, Tb, La and Ce | Waste phosphors | Alkaline fusion and leaching | Final product was $Y_2O_3$ (86.43%), $CeO_2$ (4.11%), $La_2O_3$ (3.18%), $Eu_2O_3$ (3.08%) and $Tb_4O_7$ (2.20%). The estimated total recovery of the REEs was around 70% for Y and Eu, and 80% for the others. | Innocenzi et al., (2016) |
| Y, Eu, Tb, La and Ce | Waste phosphors | Bioleaching | Total REEs leaching was low, with a maximum of ~2% for the organism B58. Y accounts for approximately 70% of the REEs in the RPP, and 80% of the REE in all of the leachates. | Reed et al., (2016) |
| Tb, Eu and Y | Waste phosphors | Mechanical activation and leaching | Due to physicochemical changes of structural destruction and particle size reduction after mechanical activation, dissolution yields were 89.4%, 93.1% and 94.6% for Tb, Eu and Y, respectively. | Tan et al., (2016) |
| Y and Eu | Pure phosphors | Leaching and ionic liquid extraction | Functionalized ionic liquid, [Hbet][$Tf_2N$], was used with ~100% Eu and Y was selectively recovered from the waste phosphor. | Dupont and Binnemans (2015) |
| Eu | Pure BAM | Alkaline fusion and leaching | Recovery of Eu was ~100% | Zhang et al., (2015) |
| Ce and Tb | Pure CTMA | Alkaline fusion and leaching | Recovery of Ce and Tb was ~100% | Liu et al., (2015) |
| Y and Eu | Waste phosphors | Leaching and extraction | Efficient leaching of Eu and Y (over 95% with 97% dissolution) was achieved. | Tunsu et al., (2014) |
| Y, Eu, Ce and Tb | Waste phosphors | Alkaline fusion and Leaching | The total leaching rate of the REEs was 94.6%. The leaching rate of Y, Eu, Ce and Tb reached 94.6%, 99.05%, 71.45%, and 76.22%, respectively. | Liu et al., (2014) |
| Ce and Tb | Waste phosphors | Alkaline fusion and Leaching | More than 99.9% of REEs were recovered. | Wu et al., (2014) |

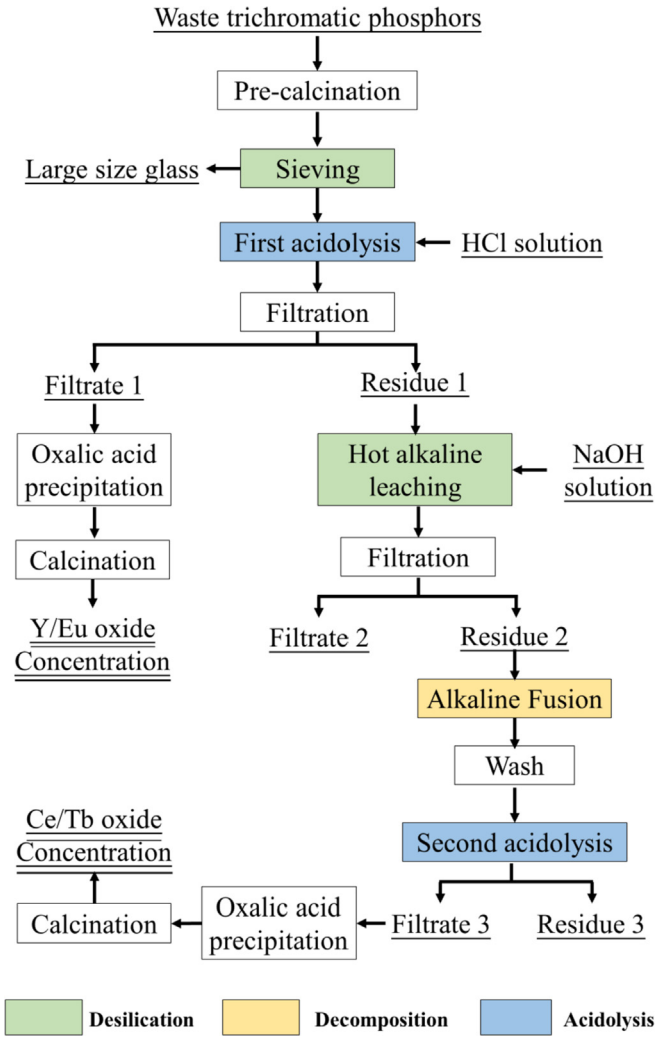


**Fig. 1.** The flow chart for recovering REEs from WTP.

### 2.3. Testing at the laboratory pilot scale

X-ray diffraction (XRD) analysis was performed using Philips APD-10 X-ray diffractometer with Cu Kα radiation, 40 kV voltage and 150 mA current at 10°/min scanning rate and 10–70° 2θ range. The morphology, aspect ratio and mean particle size were observed in the scanning electron microscope (Zeiss EVO-18, German). Chemical composition of solids was analyzed by X-ray fluorescence (XRF, Shimadzu XRF-1800, Japan). XRF provides semiquantitative analysis with the ±5% uncertainty. Chemical composition of the solution was analyzed by the inductively coupled plasma atomic emission spectroscopy (ICP-AES, PerkinElmer OPTIMA 7000DV, USA).

## 3. Results and discussion

### 3.1. Pre-calcination

Five WTP samples (100 g for each) were calcined at 200 °C, 300 °C, 400 °C, 500°, and 600 °C, respectively, for 2 h and the calcination experiment was repeated three times. The calcination temperature shows a positive effect on the removal of the organics in Fig. 2, with an increase in weight loss from 0.87 to 3.23 ± 0.1 *wt* % when the temperature was increased from 200 °C to 500 °C.

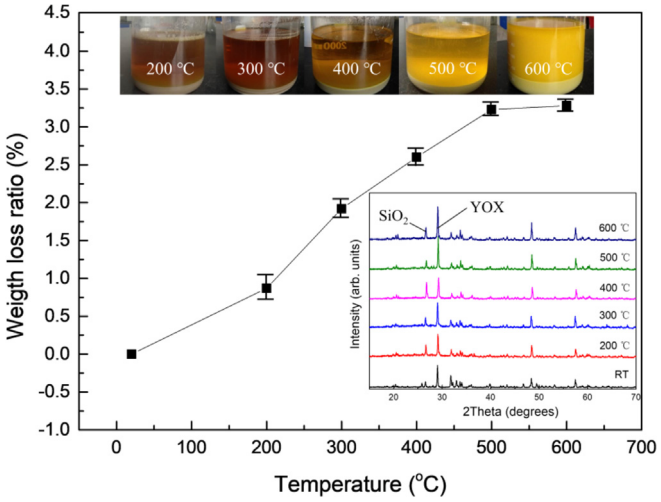


**Fig. 2.** Weight loss ratio of the waste phosphor powder baked at different temperatures.

Afterward, the effect is smaller, and the weight loss is 3.28 ± 0.05 *wt* % at 600 °C because most of organics burn off at 500 °C. The phase changes were also analyzed by XRD (inset in Fig. 2). The $SiO_2$ diffraction reflection intensity near 26° 2θ angle becomes stronger after calcination, even at 200 °C. The YOX diffraction reflection intensity near 29° 2θ angle becomes slightly stronger past 400 °C, since thermal treatment induces crystallization. The positions of X-ray diffraction reflections are not changed after calcination, which means that the main crystalline phases have not changed. More details about the main phases in WTP are shown in Fig. 3. Thermal treatment at high temperature (>400 °C) causes the formation of silica sol in the next leaching (see photos in Fig. 2), which reduces the leaching rate of Y and Eu because of absorption. Therefore, the appropriate pre-calcination temperature is 400 °C.

The chemical composition of the WTP after pre-calcination is presented in Table 1. Prior to the ICP-AES analysis, 10 g of the sample were roasted with an appropriate amount of sodium carbonate and $H_3BO_3$ at 1200 °C for 30 min, and then the product was crushed and mixed until homogeneity. 1 g of powder was dissolved in 20 ml 1M hydrochloric acid solution at 60 °C until it was completely dissolved. The solution was left to cool and diluted 1000 times with pure water (18.25 MΩ at 25 °C). Pure water was

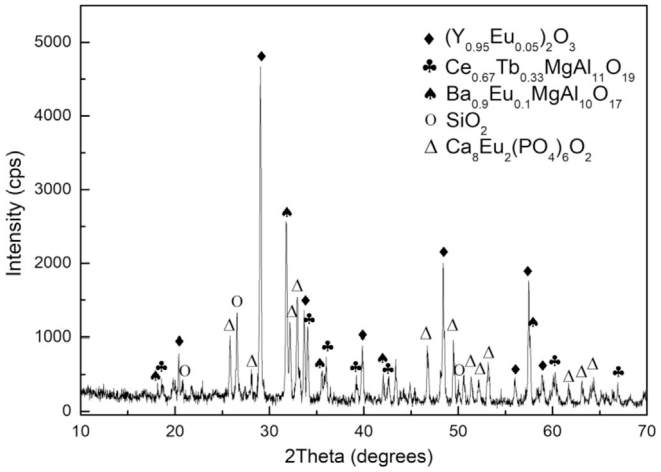


**Fig. 3.** XRD pattern of the WTP after pre-calcination at 400 °C.

**Table 2**
Chemical composition of the WTP after pre-calcination in *wt. %*.

| Heavy REEs | | | Light REEs | Harmful elements | |
|---|---|---|---|---|---|
| $Y_2O_3$ | $Tb_4O_7$ | $Eu_2O_3$ | $CeO_2$ | $SiO_2$ | $Al_2O_3$ |
| 15.9 ± 0.1 | 1.0 ± 0.05 | 1.6 ± 0.1 | 2.8 ± 0.1 | 31.8 ± 1 | 10.5 ± 0.2 |
| **Other elements** | | | | | |
| $P_2O_5$ | CaO | BaO | MgO | $Na_2O$ | $K_2O$ |
| 9.3 ± 0.2 | 13.0 ± 0.2 | 4.0 ± 0.4 | 1 ± 0.05 | 3.5 ± 0.02 | 3.7 ± 0.3 |

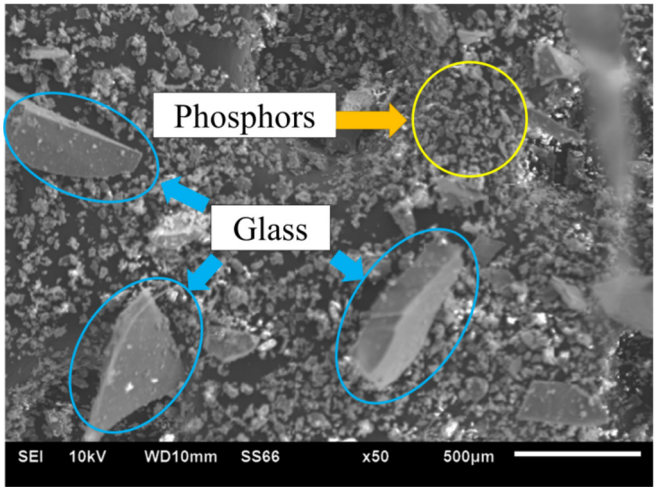


**Fig. 4.** SEM image of the WTP after pre-calcination at 400 °C.

prepared by the Aike Discovery-I device. The content was determined using ICP-AES. Standard solutions containing elements listed in Table 2 of various concentrations (0, 5, 10 and 20 ppm) were used for calibration as the internal standard. The results show that the content of REEs is ~20 *wt %* and $Y_2O_3$ is ~16% because the sample mainly contains trichromatic phosphors (Fig. 3), since the red phosphor accounts for a large percentage. However, it also has a large amount of $SiO_2$, ~32 *wt %*, as the glass was collected together during collecting WTP from waste lamps by crushing, sieving and air separation, since the density of glass is ~2.5 g/cm$^3$, which is less than WTP ($Y_2O_3$:$Eu^{3+}$: 5.1 g/cm$^3$, CTMA: 4.7 g/cm$^3$ and BAM: 3.7 g/cm$^3$), but has larger volume. Therefore, during leaching REEs, removal of glass is required in this paper.

XRD pattern of the WTP after pre-calcination at 400 °C is shown in Fig. 3. It mainly consisted of trichromatic phosphors, including YOX (JCPDS 25−1011), CTMA (JCPDS 36−0073) and BAM (JCPDS 50−0513), as well as impurities, such as $SiO_2$ (JCPDS 46−1045) and $Ca_8Eu_2(PO_4)_6O_2$ (JCPDS 33−0275). SEM analysis in Fig. 4 shows that the particles vary in size and can be larger than 500 μm or smaller than 2 μm. According to a preliminary inspection, large particles (>100 μm) with a smooth surface are glass fragments, and the small particles (<50 μm) are phosphors and fine glass, which have a tendency to form larger aggregates consisting of multiple small particles.

### 3.2. Removal of large size glass

The WTP after pre-calcination were dry sieved (38 μm, 50 μm, 74 μm, and 150 μm mesh size, respectively). Sieving results based on the size gradation and cumulative percentage passing by weight are presented in Fig. 5. The fraction consisting of particles <50 μm accounts for the bulk of the material (up to 68.4 wt %).

The XRD and SEM results of different size particles are shown in Fig. 6. The fraction <50 μm contains the majority of the phosphors powder (YOX, CTMA, and BAM, as well as $Ca_8Eu_2(PO_4)_6O_2$), and fine glass particles impurities ($SiO_2$). The other fractions contain larger glass fragments and a small amount of YOX. This is also proven by the chemical composition of different size particles in Table 3.

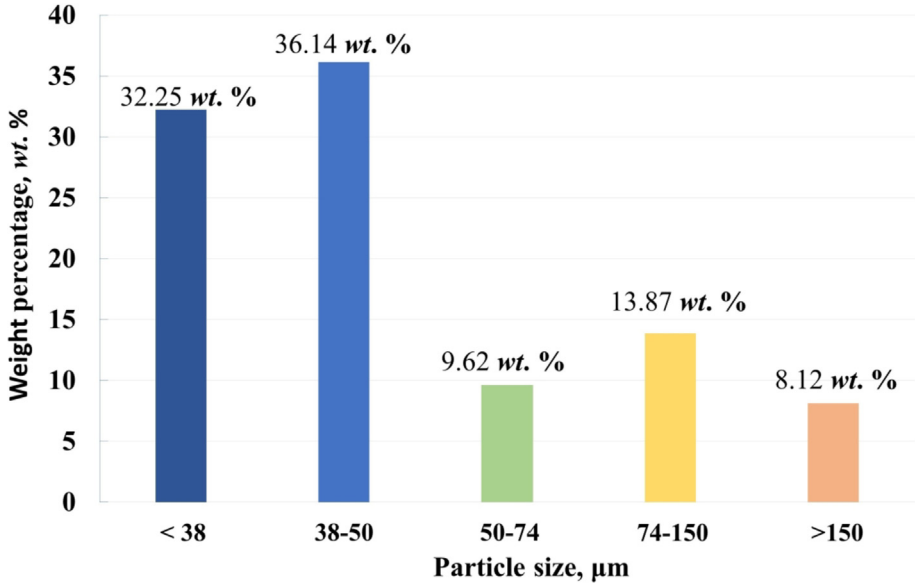


**Fig. 5.** The particle size distribution of the WTP after pre-calcination.

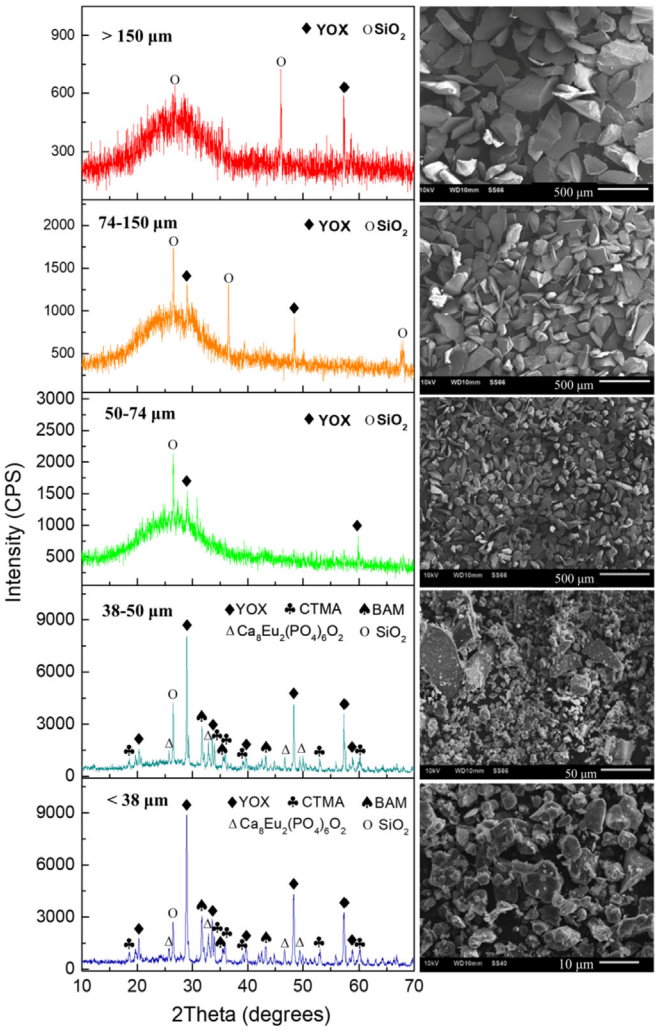


**Fig. 6.** XRD and SEM results of the different size particles.

Therefore, the large size glass can be removed by sieving with the 50 μm mesh sieve.

### 3.3. Leaching of red phosphor

Red phosphor (YOX) is the REEs oxide, which can be easily leached by HCl (4 mol/L) with the 3:1 liquid-solid ratio for 4 h with 250 rpm stirring at 60 °C (Liu et al., 2014), while part of

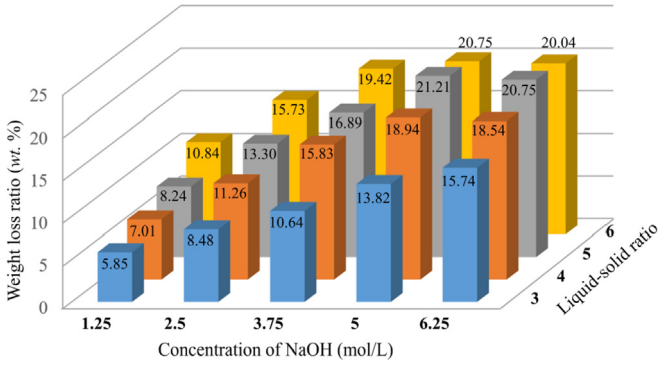


**Fig. 7.** The weight loss rate of the residue 1 treated by a hot alkaline solution at different conditions.

$Ca_8Eu_2(PO_4)_6O_2$ was also dissolved during leaching. The main chemical reactions of the first acid hydrolysis are as follows.

$$(Y_{0.95}Eu_{0.05})_2O_3 + 6HCl \rightarrow 1.9YCl_3 + 0.1EuCl_3 + 3H_2O \quad (3)$$

$$Ca_8Eu_2(PO_4)_6O_2 + 22HCl \rightarrow 8CaCl_2 + 2EuCl_3 + 6H_3PO_4 + 2H_2O \quad (4)$$

The weight loss was ~45%, and the chemical composition of the residue 1 tested by XRF is listed in Table 4.

### 3.4. Removal of fine glass

The fine glass remained in the residue 1 was dissolved in hot alkaline solution and the main chemical reaction is:

$$SiO_2 + 2NaOH \rightarrow Na_2SiO_3 + H_2O \quad (5)$$

The experiments were carried out at 90 °C and the effects of NaOH concentration and liquid-solid ratio on the weight loss are shown in Fig. 7. The weight loss is 5.85% when the NaOH concentration is 1.25 M and the liquid-solid ratio is 3, which increases with the NaOH concentration and the liquid-solid ratio. The weight loss reached ~21% when the NaOH concentration was 5 M and the liquid-solid ratio was 5, but these contributions slow down with further increase. Considering the cost, when the concentration of NaOH is 5 mol/L and the liquid-solid ratio is 5:1, the weight loss is 21 *wt %*. The weight loss increases with leaching time, but no longer increases after 4 h.

The XRD patterns of samples (residues 1 and 2) before and after hot alkaline leaching are shown in Fig. 8. After hot alkaline leaching, the intensity of the $SiO_2$ diffraction reflection significantly

**Table 3**
Chemical composition of particles with different size in *wt. %*.

| Size, μm | $Y_2O_3$ | $Eu_2O_3$ | $CeO_2$ | $Tb_4O_7$ | $SiO_2$ | $Al_2O_3$ | CaO | $P_2O_5$ | BaO | $K_2O$ | $Na_2O$ | MgO |
|---|---|---|---|---|---|---|---|---|---|---|---|---|
| <50 | 22.9 | 2.3 | 4.0 | 1.5 | 17.2 | 13.5 | 15.8 | 13.3 | 2.7 | 2.2 | 1.4 | 1.5 |
| 50–74 | 1.3 | – | – | – | 61.2 | 4.2 | 8.6 | 0.9 | 7.3 | 6.8 | 7.8 | 0.1 |
| 74–150 | 0.6 | – | – | – | 64.3 | 3.9 | 6.6 | 0.7 | 6.6 | 7.2 | 8.1 | 0.2 |
| >150 | 0.5 | – | – | – | 64.6 | 3.7 | 6.2 | 0.5 | 6.7 | 7.3 | 8.6 | 0.2 |

-, not detected.

**Table 4**
Chemical composition of the residue 1 in *wt. %*.

| $Y_2O_3$ | $Eu_2O_3$ | $CeO_2$ | $Tb_4O_7$ | $SiO_2$ | $Al_2O_3$ | CaO | $P_2O_5$ | BaO | $K_2O$ | $Na_2O$ | MgO | Others |
|---|---|---|---|---|---|---|---|---|---|---|---|---|
| 1.6 | – | 7.3 | 2.8 | 31.3 | 25.3 | 7.8 | 6.2 | 5.1 | 4.0 | 2.7 | 2.6 | 3.3 |

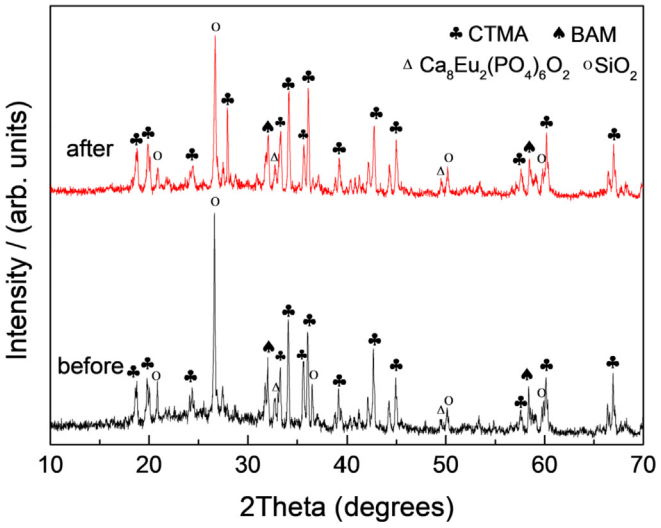


**Fig. 8.** XRD patterns of the residues 1 and 2 before and after hot alkaline leaching.

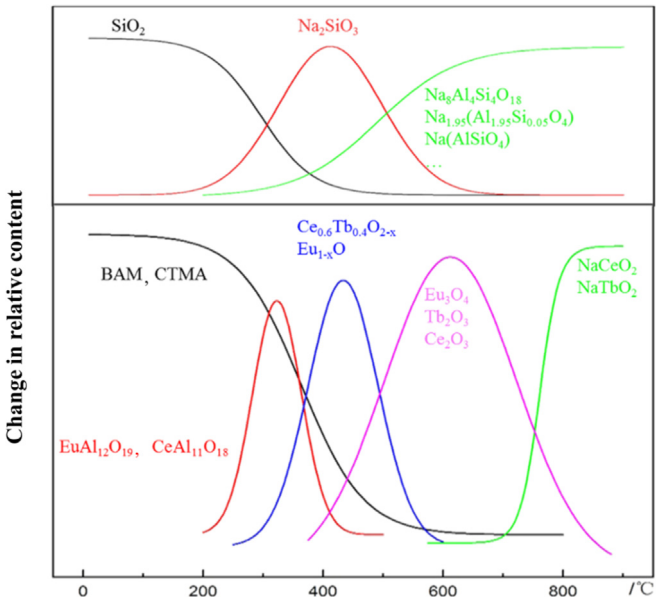


**Fig. 9.** Phase transformations during alkaline fusion at different temperatures.

decreases near 26°, and part of the amorphous silicon diffraction reflection disappeared between 20° and 40°. The diffraction intensity of BAM decreases near 32° and 58° 2θ angles. This means that most of $SiO_2$ and maybe a small amount of BAM are dissolved in the hot alkaline fusion. However, the diffraction reflection of CTMA has barely changed. The chemical composition of the residue 1 tested by XRF is listed in Table 5. The $SiO_2$ content reduced to 13 *wt %* from 31 *wt %*. These results showed that most of the fine $SiO_2$ was further removed by hot alkaline leaching. Finally, approximately 88% of glass fragments in the original matrix were removed after two steps desilication process.

### 3.5. Decomposition of blue and green phosphors

In the previous study, CTMA and BAM were decomposed to acid-soluble oxides following reactions (6) and (7). However, the residual fine $SiO_2$ causes complicated reactions (8–10), based on the XRD data of alkaline fusion products at different temperature. Since the diffraction data is complicated, the phase transformations are summarized in Fig. 9. BAM (Zhang et al., 2015) and CTMA begin to decompose at 250 °C (Liu et al., 2015), and the interim phases were $EuAl1_2O_{19}$ and $CeAl_{11}O_{15}$, while the $Na_2SiO_3$ phase was generated. When the temperature increased to 450 °C, the main phases were REO and $NaAlO_2$. However, above 600 °C, the $NaAlO_2$ reacts with $Na_2SiO_3$ to generate complicated aluminosilicates, such as $Na_2SiO_3$, $Na_{1.95}(Al_{1.95}Si_{0.05}O_4)$, and $Na(AlSiO_4)$. The REO changed to $NaREO_2$ at 800 °C, and since it is water-soluble, it would reduce the recovery of REEs during next washing (Liu et al., 2014).

$$BAM + NaOH + CO_2 \rightarrow NaAlO_2 + MgO + BaCO_3 + Eu_2O_3 + H_2O \quad (6)$$

$$CTMA + NaOH \rightarrow NaAlO_2 + MgO + CeO_2 + Tb_2O_3 + H_2O \quad (7)$$

$$SiO_2 + 2NaOH \rightarrow Na_2SiO_3 + H_2O \quad (8)$$

$$NaAlO_2 + SiO_2 \rightarrow Na(AlSiO_4) \quad (9)$$

$$1.95NaAlO_2 + 0.05SiO_2 + O_2 \rightarrow Na_{1.95}(Al_{1.95}Si_{0.05}O_4) \quad (10)$$

Therefore, in order to decompose BAM and CTMA, but avoid generating complicated aluminosilicate, the residue 1 and NaOH were mixed at the 1:1 mass ratio. Sintering was performed at 600 °C for 2 h.

The product was washed by deionized water several times to remove excess NaOH, $NaAlO_2$, and part of $Na_2SiO_3$. Next, the washed product was leached with HCl (5 mol/L) for 2 h with 250 rpm stirring at 60 °C and the liquid-solid ratio was 5:1. During the acidolysis, the REOs were dissolved as $RECl_x$ ($x = 3$ *or* $4$) by HCl, following reactions (11).

$$CeO_2 + Tb_2O_3 + 10\ HCl \rightarrow CeCl_4 + 2\ TbCl_3 + 5\ H_2O \quad (11)$$

After filtration, the filtrate 3 (Tb–Ce chloride concentrate) was obtained. Y–Eu and Ce–Tb oxides are then treated with oxalic acid at 70–80 °C and 1.8–2.1 pH to precipitate REE oxalates, which are subsequently thermally treated at 800 °C to obtain oxides. The final product obtained with the described process was a mixture of REEs oxides, which could be further treated to selectively recover the solo REE by solvent extraction.

### 3.6. The leaching rate

Under the above appropriate conditions, 200 g of waste phosphors after pre-calcination were used as the raw materials. Since the uncertainty of XRF is ±5%, the REEs content of the filtrate 1 (Y–Eu rich solution) and 3 (Tb–Ce rich solution) tested by ICP-AES were used to calculate the leaching rates in Table 6. The total REOs leaching rate was 94%. Meanwhile, the leaching rate of Y, Eu, Ce, and Tb reached 96%, 99%, 81%, and 92%, respectively. Most of the $SiO_2$ had been removed, but it is hard to remove it completely. It cannot

**Table 5**
Chemical composition of the residue 2 in *wt. %*.

| $Y_2O_3$ | $Eu_2O_3$ | $CeO_2$ | $Tb_4O_7$ | $SiO_2$ | $Al_2O_3$ | CaO | $P_2O_5$ | BaO | $K_2O$ | $Na_2O$ | MgO |
|---|---|---|---|---|---|---|---|---|---|---|---|
| 1.5 | 0 | 9.0 | 3.4 | 13.3 | 31.7 | 9.8 | 7.8 | 6.4 | 4.9 | 5.4 | 3.3 |

**Table 6**
REEs content of the filtrates 1 and 3.

| REEs content, g | $Y_2O_3$ | $Eu_2O_3$ | $CeO_2$ | $Tb_4O_7$ |
|---|---|---|---|---|
| Filtrate 1 | 30.12 ± 1.5 | 3.06 ± 0.2 | – | – |
| Filtrate 3 | 0.46 ± 0.02 | 0.04 ± 0.002 | 4.27 ± 0.21 | 1.91 ± 0.05 |
| Total | 30.58 ± 1.5 | 3.10 ± 0.2 | 4.27 ± 0.21 | 1.91 ± 0.05 |
| Waste phosphors | 31.88 ± 1.5 | 3.14 ± 0.2 | 5.30 ± 0.26 | 2.08 ± 0.05 |
| **Leaching rate, %** | 96 | 99 | 81 | 92 |
| **Total rate, %** | **94** | | | |

be totally avoided that the Ludox particles adsorbed RE ions. Therefore, the leaching rate of Ce and Tb was lower than Y and Eu.

## 4. Sustainability

### 4.1. Saving auxiliary materials and energy

The existing process of recycling waste phosphors in Chinese factories includes three steps. (1) Remove large glass fragments, but ignore the fine glass. (2) Decompose the phosphors by alkaline fusion at about 800 °C. (3) Remove excessive alkali and $NaAlO_2$ by washing, then leach rare earth elements from the alkaline fusion products. There are two cons: (1) compared with the existing commercial process, red phosphor with other phosphors react with NaOH in the alkaline fusion process. However, the red phosphor transforms into $NaYO_2$. This causes the loss of Y in the following washing process. However, in this paper, this loss can be avoided, since red phosphor was dissolved in the first acid hydrolysis, and almost all of Y was recovered in the filtrate 1 (Liu et al., 2014). (2) Fine glass becomes aluminosilicate and generates silica gel during leaching, which is the main reason for the low REEs leaching rate. Therefore, two-step acidolysis and desilication were designed. Compared with the new process in the paper, it has a higher cost of auxiliary materials and energy, but a lower recovery of about 50%.

In the industrial trial, 1000 kg trichromatic phosphors containing glass was used as raw material. The statistics of the cost of auxiliary materials and energy recorded from pilot plant research are listed in Table 7. According to the comparison of the auxiliary materials cost and energy, this approach increased the REEs recovery to 90%, although the process route is more complicated. There are two major reasons. (1) Selective leaching of YOX before alkaline fusion, which avoids the loss of Y during washing, since YOX is easily transformed into water-soluble $NaYO_2$ during alkaline fusion. (2) Desilication decreasing the amount of colloidal silica, which can adsorb REEs ions during leaching. Additionally, the use of water, hydrochloric acid, and sodium hydroxide is saved by 40%, 5%, and 34%, and the consumption of coal and electricity is additionally reduced by 34% and 8%, respectively. The leaching efficiency is increased by the two-step acidolysis, which also decreases the content of impurities and glass, consuming less unnecessary auxiliary materials and energy.

**Table 8**
The operating costs and the revenues from the one-ton waste phosphors.

| Feature | € | Share, % |
|---|---|---|
| Operating costs | | |
| Raw materials | 1260 | 40.76 |
| Pre-calcination | 30 | 0.97 |
| Removal of large size glass | 10 | 0.32 |
| Leaching of red phosphor | 6 | 0.19 |
| Removal of fine glass | 154 | 4.98 |
| Decomposition of blue and green phosphors | 192 | 6.21 |
| Washing | 1 | 0.03 |
| Leaching of blue and green | 2 | 0.06 |
| Precipitation and calcination | 461 | 14.91 |
| Solvent extraction | 513 | 16.60 |
| Precipitation and calcination | 461 | 14.91 |
| **Total** | **3090** | **100** |
| **Revenues** | | |
| $Tb_4O_7$ (99.9%) | 3310 | 78.72 |
| $Eu_2O_3$(99.5%) | 503 | 11.96 |
| $Y_2O_3$(99.99%) | 356 | 8.47 |
| $CeO_2$(99.5%) | 36 | 0.86 |
| **Total** | **4205** | **100** |

### 4.2. Economic assessment

The economic assessment provides the operating costs (including raw materials, utilities, maintenance, labor, fixed and general, overhead and capital depreciation) and revenues for one-ton waste phosphors in China (Table 8). The price of raw materials depends on the content of REEs and impurities, which is normally 30–80% of the total value of REEs. In this paper, the purchasing cost of raw materials is around 30% market price of the REOs in the waste phosphors, because it has low content of high valuable REEs (Tb and Eu), but large amount of glass. The cost of raw materials accounts for the vast majority proportion of the total cost, followed by the purification process, including solvent extraction (16.6%), precipitation and calcination (29.8%), which require expensive organic reagents and more energy. The cost proportion of removal of fine glass and decomposition of blue and green phosphors is 4.98% and 6.21%, respectively. The others are

**Table 7**
The comparison of the cost of auxiliary materials and energy.

| | Water, L | HCl, 10M, L | NaOH, Kg | Energy | | Recovery, % |
|---|---|---|---|---|---|---|
| | | | | Coal, kg | Electricity, kWh | |
| The approach in this work | | | | | | |
| 1st acidolysis | 2000 | 1200 | – | 30.91 | 26.50 | 90 |
| Remove fine glass | 3000 | – | 550 | 6.90 | 17.33 | |
| Alkaline fusion | | – | 433 | 42.24 | 6 | |
| Washing | 9000 | – | – | – | | |
| 2nd acidolysis | 2600 | 1175 | – | 23.73 | 8.17 | |
| **Total** | **16400** | **2375** | **983** | **103.78** | **58** | |
| Existing commercial process | | | | | | |
| Alkaline fusion | | – | 1500 | 97.53 | 18 | 50 |
| Washing | 22000 | | | | | |
| Acidolysis | 5500 | 2500 | – | 60.18 | 45 | |
| Total | 27500 | 2500 | 1500 | 157.71 | 63 | |
| **Savings, %** | **40** | **5** | **34** | **34** | **8** | |

less than 1%. Revenues of production are calculated based on the latest price of rare earth oxides (February 2019). From the revenues, the value of $Tb_4O_7$ is the highest, accounting for 78.72% of all revenues. Except for the fixed capital investment and taxes, it shows a positive value for this approach, which implies economic feasibility, since the benefit is 1115 €/ton.

### 4.3. Balance of supply and demand

China is by far the world's largest producer and consumer of rare earth elements, supplying around 80% of the globe's rare earth needs. Due to the socio-environmental issues and the health impact, the Chinese government has drastically cut back on domestic production of rare earth minerals (McLellan et al., 2014). This causes exports to oscillate wildly from month to month. In the first half of 2018, the figure was 70,000 tons, 40% higher than the first half of 2017, but it reduced to 45,000 tons in the second half of 2018. Before exporting, China is likely to attend to its own needs. However, REEs will remain critical for future generations, allowing for further improvements in product miniaturization, performance and efficiency. Therefore, the approach presented in this paper makes it possible to supply REEs outside of China through recycling of REEs from waste trichromatic phosphors.

## 5. Conclusions

The desilication, decomposition, and acidolysis were used to recycle rare earth elements from real waste trichromatic phosphors containing glass at laboratory and pilot plant scales. The effects of sieving, alkaline leaching conditions and alkaline fusion temperature on removal of glass and recycling of REEs were investigated.

1. 88% of glass fragments were removed after dry sieving through a 0.05 mm mesh sieve and leaching by 5 mol/L NaOH solution at 90 °C for 4 h with the appropriate 5:1 liquid-solid ratio.
2. The total leaching rate of rare earth elements reached 94%, while the rates of yttrium, europium, cerium, and terbium were 96%, 99%, 81%, and 92%, respectively.
3. Compared with the existing technology in China, the application of this approach increased the recovery of REEs from 50% to 90%.
4. Except for the fixed capital investments and taxes, it shows a positive value for this approach, which implies economic feasibility, since the benefit is 1115 €/ton.

Therefore, the recycling of REEs from waste phosphors is one of the cleaner and economical way to balance the supply and demand of REEs outside of China.

## Acknowledgments

The authors gratefully acknowledge the support provided by the Youth Natural Science Foundation of the Jiangxi Province (Grant No. 20181BAB216025) and the Project of the Xijiang Innovation Team.

## References

Ali, S.H., Giurco, D., Arndt, N., Nickless, E., Brown, G., Demetriades, A., Durrheim, R., Enriquez, M.A., Kinnaird, J., Littleboy, A., Meinert, L.D., Oberhänsli, R., Salem, J., Schodde, R., Schneider, G., Vidal, O., Yakovleva, N., 2017. Mineral supply for sustainable development requires resource governance. Nature 543 (7645), 367.
Aljerf, L., Al Masri, N., 2018. Mercury toxicity: ecological features of organic phase of mercury in biota-Part I. Arch. Org. Inorg. Chem. Sci. 3 (3), 1–8.
Balaz, P., Achimovicova, M., Balaz, M., Billik, P., Cherkezova-Zheleva, Z., Criado, J.M., Delogu, F., Dutkova, E., Gaffet, E., Gotor, F.J., Kumar, R., Mitov, I., Rojac, T., Senna, M., Streletskii, A., Wieczorek-Ciurowa, K., 2013. Hallmarks of mechanochemistry: from nanoparticles to technology. Chem. Soc. Rev. 42 (18), 7571–7637.
Binnemans, K., Jones, P.T., Blanpain, B., Van, Gerven, T., Pontikes, Y., 2015. Towards zerowaste valorisation of rare-earth-containing industrial process residues: a critical review. J. Clean. Prod. 99, 17–38.
Chang, T.C., You, S.J., Yu, B.S., Chen, C.M., Chiu, Y.C., 2009. Treating high-mercury containing lamps using full-scale thermal desorption technology. J. Hazard. Mater 162, 967–972.
Coradin, T., Durupthy, O., Livage, J., 2002. Interactions of amino-containing peptides with sodium silicate and colloidal silica: a biomimetic approach of silicification. Langmuir 18 (6), 2331–2336.
Coskun, S., Civelekoglu, G., 2015. Recovery of mercury from spent fluorescent lamps via oxidative leaching and cementation. Water Air. Soil Pollut. 226, 1–13.
Dupont, D., Binnemans, K., 2015. Rare-earth recycling using a functionalized ionic liquid for the selective dissolution and revalorization of $Y_2O_3$:$Eu^{3+}$ from lamp phosphor waste. Green Chem. 17, 856–868.
European Commission, 2017. Report on Critical Raw Materials for the EU. http://ec.europa.eu/growth/sectors/raw-materials/specific-interest/critical_en.
Goodenough, K.M., Wall, F., Merriman, D., 2018. The rare earth elements: demand, global resources, and challenges for resourcing future generations. Nat. Resour. Res. 27 (2), 201–216.
Hasegawa, H., Begum, Z.A., Murase, R., Ishii, K., Sawai, H., Mashio, A.S., Maki, T., Rahman, I.M., 2018. Chelator-induced recovery of rare earths from end-of-life fluorescent lamps with the aid of mechano-chemical energy. Waste Manag. 80, 17–25.
He, L., Ji, W., Yin, Y., Sun, W., 2018. Study on alkali mechanical activation for recovering rare earth from waste fluorescent lamps. J. Rare Earths 36 (1), 108–112.
Hopfe, S., Konsulke, S., Barthen, R., Lehmann, F., Kutschke, S., Pollmann, K., 2018. Screening and selection of technologically applicable microorganisms for recovery of rare earth elements from fluorescent powder. Waste Manag. 79, 554–563.
Hopfe, S., Flemming, K., Lehmann, F., Möckel, R., Kutschke, S., Pollmann, K., 2017. Leaching of rare earth elements from fluorescent powder using the tea fungus Kombucha. Waste Manag. 62, 211–221.
Innocenzi, V., Ippolito, N.M., Pietrelli, L., Centofanti, M., Piga, L., Veglio, F., 2018. Application of solvent extraction operation to recover rare earths from fluorescent lamps. J. Clean. Prod. 172, 2840–2852.
Innocenzi, V., Ippolito, N.M., De Michelis, I., Medici, F., Veglio, F., 2016. A hydrometallurgical process for the recovery of terbium from fluorescent lamps: experimental design, optimization of acid leaching process and process analysis. J. Environ. Manag. 184 (3), 552–559.
Ippolito, N.M., Innocenzi, V., De Michelis, I., Medici, F., Veglio, F., 2017. Rare earth elements recovery from fluorescent lamps: a new thermal pretreatment to improve the efficiency of the hydrometallurgical process. J. Clean. Prod. 153, 287–298.
Jang, M., Hong, S.M., Park, J.K., 2005. Characterization and recovery of mercury from spent fluorescent lamps. Waste Manage 25, 5–14.
Jowitt, S.M., Werner, T.T., Weng, Z., Mudd, G.M., 2018. Recycling of the rare earth elements. Curr. Opin. Green Sustain. Chem. 13, 1–7.
Kumari, A., Jha, M.K., Pathak, D.D., 2018. March. Review on the processes for the recovery of rare earth metals (REMs) from secondary resources. In: TMS Annual Meeting & Exhibition. Springer, Cham, pp. 53–65.
Lederer, F.L., Curtis, S.B., Bachmann, S., Dunbar, W.S., MacGillivray, R.T., 2017. Identification of lanthanum-specific peptides for future recycling of rare earth elements from compact fluorescent lamps. Biotechnol. Bioeng. 114 (5), 1016–1024.
Liu, H., Zhang, S.G., Pan, D.A., Tian, J.J., Yang, M., Wu, M.L., Volinsky, Alex A., 2014. Rare earth elements recycling from waste phosphor by dual hydrochloric acid dissolution. J. Hazard Mater. 272, 96–101.
Liu, H., Zhang, S.G., Pan, D.A., Liu, Y.F., Liu, B., Tian, J.J., Volinsky, Alex A., 2015. Mechanism of $CeMgAl_{11}O_{19}$:$Tb^{3+}$ alkaline fusion with sodium hydroxide. Rare Met. 34 (3), 189–194.
Mancheri, N.A., 2015. World trade in rare earths, Chinese export restrictions, and implications. Resour. Policy 46, 262–271.
McLellan, B.C., Corder, G.D., Golev, A., Ali, S.H., 2014. Sustainability of the rare earths industry. Procedia Environ. Sci. 20, 280–287.
Pellegrini, M., Godlewska, L., Millet, P., Gislev, M., Grasser, L., 2017. EU potential in the field of rare earth elements and policy actions. An ERES 12–15.
Reed, D.W., Fujita, Y., Daubaras, D.L., Jiao, Y., Thompson, V.S., 2016. Bioleaching of rare earth elements from waste phosphors and cracking catalysts. Hydrometallurgy 166, 34–40.
Tan, Q., Deng, C., Li, J., 2016. Innovative applications of mechanical activation for rare earth elements recovering: process optimization and mechanism exploration. Sci. Rep. 6, 19961.
Tang, J., Qiao, J., Xue, Q., Liu, F., Chen, H., Zhang, G., 2018. Leach of the weathering crust elution-deposited rare earth ore for low environmental pollution with a combination of $(NH_4)_2SO_4$ and EDTA. Chemosphere 199, 160–167.
Tanaka, M., Oki, T., Koyama, K., Narita, H., Oishi, T., 2013. Recycling of Rare Earths from Scrap in Handbook on the Physics and Chemistry of Rare Earths, vol. 43, pp. 159–212.
Tunsu, C., Ekberg, C., Retegan, T., 2014. Characterization and leaching of real fluorescent lamp waste for the recovery of rare earth metals and mercury. Hydrometallurgy 145, 91–98.
Tunsu, C., Ekberg, C., Foreman, M., Retegan, T., 2015. Investigations regarding the wet decontamination of fluorescent lamp waste using iodine in potassium iodide solutions. Waste Manag. 36, 289–296.

Tunsu, C., Petranikova, M., Ekberg, C., Retegan, T., 2016. A hydrometallurgical process for the recovery of rare earth elements from fluorescent lamp waste fractions. Separ. Purif. Technol. 161 (17), 172–186.
Van Loy, S., Binnemans, K., Van Gerven, T., 2018. Mechanochemical-assisted leaching of lamp phosphors: a green engineering approach for rare-earth recovery. Engineering 4 (3), 398–405.
Wu, Y., Wang, B., Zhang, Q., Li, R., Sun, C., Wang, W., 2014. Recovery of rare earth elements from waste fluorescent phosphors: $Na_2O_2$ molten salt decomposition. J. Mater. Cycles Waste 16 (4), 635–641.
Yu, M.M., Mei, G.J., Chen, X.D., 2018. Recovering rare earths and aluminum from waste $BaMgAl_{10}O_{17}$: $Eu^{2+}$ and $CeMgAl_{11}O_{19}$:$Tb^{3+}$ phosphors using NaOH submolten salt method. Miner. Eng. 117, 1–7.
Zhang, S., Liu, H., Pan, D.A., Tian, J., Liu, Y., Volinsky, A.A., 2015. Complete recovery of Eu from $BaMgAl_{10}O_{17}$: $Eu^{2+}$ by alkaline fusion and its mechanism. RSC Adv. 5 (2), 1113–1119.